Supplementary Material 1: Infrared spectra and peak assignments for Cladophora aegagropila cellulose fibrils

Spatiotemporal dynamics of cellulose during enzymatic hydrolysis studied by infrared spectromicroscopy

Tina Jeoh[1,*], Jennifer Danger Nill[1,2,§], Wujun Zhao[3,4,§], Sankar Raju Narayanasamy[3,5,§], Liang Chen[3,6], and Hoi-Ying N. Holman[3,*]
[§] These authors contributed equally to this manuscript
[1]Biological and Agricultural Engineering, University of California Davis, Davis, CA
[2]Current: Amyris, Emeryville, CA
[3]Berkeley Synchrotron Infrared Structure Biology (BSISB), Lawrence Berkeley National Lab (LBNL), Berkeley, CA
[4]Current: Genus IntelliGen Technologies, Windsor, Wisconsin
[5]Current: Biosciences and Biotechnology Division, Physical and Life Science, Lawrence Livermore National Laboratory, Livermore, CA
[6]Current: TikTok, Mountain View, California

[*]Corresponding Authors

The sFTIR spectra of cellulose feature signature absorbance peaks in the hydrogen bonding (~3200 - 3500 cm^{-1}), -CH vibration (~2800 – 3000), and the fingerprint regions (~900 – 1500 cm^{-1}) (Figure S1. 1). Consistent with previous reports, the fingerprint region of the cellulose sFTIR spectrum show strong absorbance peaks due to C-O bond vibrations at the 2nd, 3rd and 6th carbons of the glucose residues of cellulose (C2, C3 and C6, respectively) centered at ~ 1111 cm^{-1} and 1124 cm^{-1}, 1060 cm^{-1}, and 1033 cm^{-1}, respectively (Figure S1. 1A). The asymmetric and symmetric stretching of the –C-O-C ether bond of the glycosidic bond in cellulose absorb maximally near 1160 cm^{-1} and 1205 cm^{-1}, respectively (Marechal & Chanzy, 2000). The asymmetric stretching peak of the glycosidic bond at ~ 1160 cm^{-1} is dominant and commonly used as a diagnostic marker for cellulose. Additionally, a shoulder peak centered at ~1153 cm^{-1} attributed to C-O stretching of the anomeric carbon (Nikonenko et al., 2000) can be seen in the spectra. The corresponding identification of the C-O stretch at the 4th carbon (i.e. non-reducing ends of cellulose) is not commonly identified in the literature. A minor peak centered at ~1086 cm^{-1} (peak 7) is a possible candidate for C4-O vibration. The small peak size comparable to the shoulder at 1153 cm^{-1} of the reducing-end, and the location between the C3-O and C2-O peaks, where C2-OH, C3-OH, and C4-OH are secondary alcohols, lend support to this hypothetical assignment.

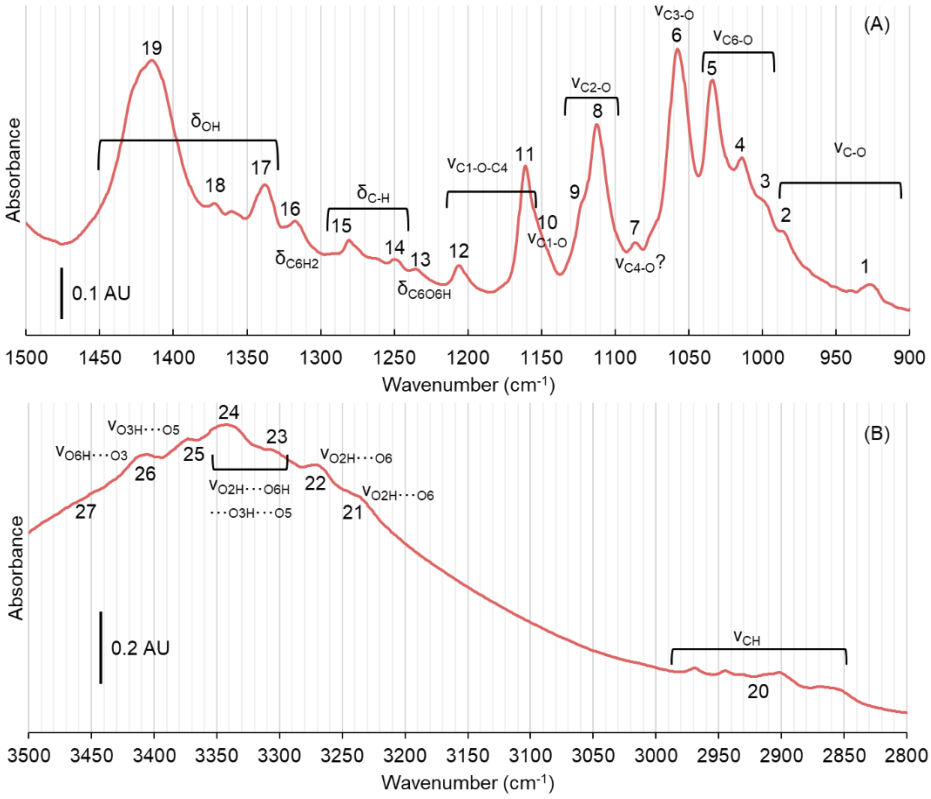

Figure S1. 1: sFTIR spectra of cellulose in sodium acetate buffer A) in the fingerprint region (900 – 1500 cm^{-1}) characterized by absorption due to C-O vibration, C-H bending and O-H bending; B) in the '–CH' and 'hydrogen bonding' region (2800 – 3500 cm^{-1}) characterized by absorption due to C-H vibration, and –OH vibration peaks of cellulose. Numbered peaks are tabulated inTable S1. 1. An illustration of cellulose identifying C-O bonds and hydrogen bonding patterns is shown in Figure S1. 2.

Corresponding to the C-O stretches are –OH vibration peaks that occur in the 3200 – 3500 cm^{-1} frequency range (Figure S1. 1B). Peak assignment in this range has undergone considerable refinement over the years as new information on the crystalline morphology and hydrogen bonding patterns in cellulose come to light (Lee et al., 2015; Liang & Marchessault, 1959; Marechal & Chanzy, 2000; Schwanninger et al., 2004). While some uncertainty remains, this work uses peak assignments with general and broad consensus. The lowest frequency peaks in the spectra of hydrated cellulose centered at ~ 3240 and 3270 cm^{-1} (Figure S1. 1B) are assigned to intramolecular hydrogen bonds formed by O2H of one glucose residue and O6 of the neighboring glucose residue (Figure S1. 2). Lee et al. (Lee et al., 2015) suggest that the O2H···O6 hydrogen bonds of cellulose Iα absorbs maximally near 3240 cm^{-1}, while those of cellulose Iβ absorbs maximally near 3270 cm^{-1}. The cellulose used in this study, isolated from the cell walls of the macroalgae, *Cladophora aegagropila*, is predominantly cellulose Iα (O'Dell et al., 2015). Contrary to Lee et al.'s rationale, the 3240 cm^{-1} peak is of lower intensity than at 3270 cm^{-1}, suggesting a lower abundance of the cellulose Iα morphology. An alternate explanation is that the two O2H-O6 hydrogen bonding peaks correspond to the two C2-O peaks observed ~1111 cm^{-1} and 1124 cm^{-1} in the fingerprint region. The O2H···O6 hydrogen bonds are the strongest in the cellulose fibrils, as evidenced by the lowest frequency absorption of these peaks. Along with the O3H···O5 hydrogen bonds, the O2H···O6 hydrogen bonds flank on either side of the glycosidic bond (Figure S1. 2), which increases the stiffness of the glucan chain (Nishiyama, 2009). Moreover, the O2H···O6 hydrogen bonds are proposed to be the origin on the right-handed twisting of cellulose I (Bu et al., 2015).

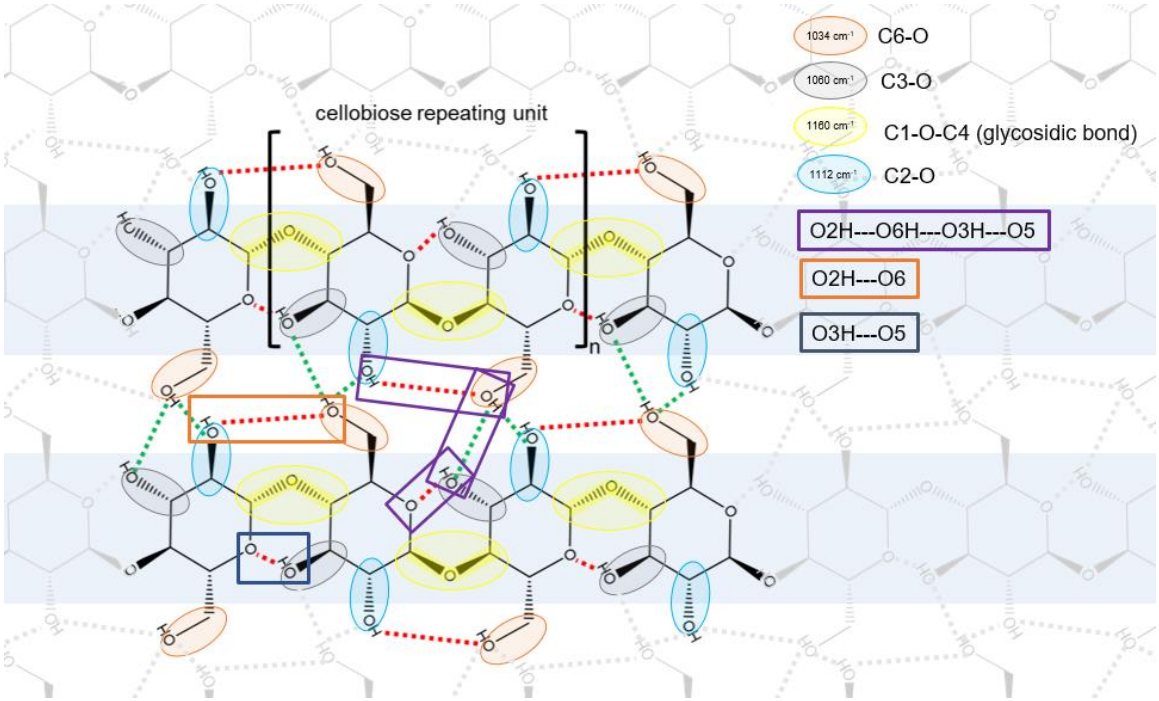

Figure S1. 2: Illustration of the C-O bonds and hydrogen bonding patterns characteristic of cellulose I. Red dotted lines indicate intramolecular hydrogen bonds; Green dotted lines indicate intermolecular hydrogen bonds.

The hydroxymethyl group at C6 along the cellulose backbone can rotate about the C5-C6 bond in each glucose residue and occupy three dominant rotameric forms (Matthews et al., 2006). The ratio of the three rotamers at the cellulose surfaces strongly depends on the nature of the solvent, while the trans-gauche (*tg*) rotameric form facilitating intramolecular hydrogen bonds between C6O6 and O2H dominate within the fibril structures of cellulose I (Matthews et al., 2006; Shen & Gnanakaran, 2009). The *tg* rotamer also facilitates intermolecular hydrogen bonding between O6H of one cellulose molecule and O3 of the adjacent molecule. In the IR spectra, the coordination of hydrogen bonds across O2H···O6H···O3H···O5 (Figure S1. 2) contribute to maximum absorption in the range of ~3300 – 3350 cm^{-1} (Lee et al., 2015). In this work, peaks centered near 3305 and 3345 cm^{-1} were observed and assigned to the O2H···O6H···O3H···O5 hydrogen bonds (Figure S1. 1B and Table S1. 1).

Peaks at around 3375 cm^{-1} and 3405 cm^{-1} are assigned to the O3H···O5 and O6H···O3 hydrogen bonds, respectively. As mentioned, the O3H···O5 hydrogen bonds brace the glycosidic bonds along with the O2H···O6 hydrogen bonds. The higher frequency absorption of the O3H···O5 hydrogen bonds indicate that these are weaker than the O2H···O6 hydrogen bonds, lending support to Bu et al.'s (Bu et al., 2015) proposal that the O2H···O6 hydrogen bonds, rather than the O3H···O5 hydrogen bonds are responsible for the twist in cellulose I. Peak assignments are summarized in Table S1. 1.

Table S1. 1: Peak assignment in the FTIR spectra of dry and hydrated cellulose.

Peak # [1]	***Peak Center [2] (cm^{-1})***	***Bond Assignment***	***Cellulose Structural Feature [3]***	***Intra-fibril hydrogen bonding [4]***
-	895 – 896	γCOC at β-glycosidic linkage	Amorphous region	
1	924	γ ring vibration		
2	984 – 985	νC-O		
3	998	νC-O	C6-O6 *gt*-rotamer (minor)	
4	1012	νC-O	C6-O6 *gg*-rotamer (secondary)	
5	1034	νC-O	C6-O6 *tg*-rotamer (primary)	Intra: O6-HO2 Inter: O6H-O3, O6H-O2
6	1059	νC-O	C3-O3	Intra: O3H-O5 Inter: O3-HO6
7	1086	νC-O	C4-O4? Non-reducing end?	
8	1112	νC-O	C2-O2	Weak/no H-bond
9	1124	νC-O	C2-O2	Inter: O6-HO2
10	1153	νC-O	C1-O1 Anomeric carbon	
11	1161	ν_SC-O-C	Glycosidic bond	
12	1206	ν_{AS}C-O-C	Glycosidic bond	
13	1236	δC-O-H	C6-O6	Intra: O6-HO2 Inter: O6H-O3, O6H-O2
14	1250	δC-H		
15	1281	δC-H		
16	1315	δCH_2	H-C6-H	
17	1340	δOH	O2H and O3H	

18	1372	δOH		
19	1429	δOH	crystalline region C6-O6H	
20	~2840~ 2980	νCH		
21	~3230	νO-H	O2-H Cellulose Iα[5]	Intra: C2O2H-O6
22	~3268	νO-H	O2-H Cellulose Iβ[5]	Intra: C2O2H-O6
23	3305	νO-H	Coupled inter and intra hydrogen bonds	O2H-O6H-O3H-O5
24	3345	νO-H	Coupled inter and intra hydrogen bonds	O2H-O6H-O3H-O5
25	3375	νO-H		Intra: O3H-O5
26	3405	νO-H		Inter: O6H-O3
27	3450	νO-H		Weak or no H-bonds (TG>GT>GG)[5]

[1] Peak numbering in the hydrated cellulose spectra shown in Figure S1. 1.
[2] Hydrated in sodium acetate buffer.
[3] Peak assignments based on previous work (Fan et al., 2012; Kondo & Sawatari, 1996; Lee et al., 2015; Marechal & Chanzy, 2000; Nikonenko et al., 2000; R. Stuart Tipson, 1968)
[4] Intramolecular (Intra) and intermolecular (Inter) molecular hydrogen bonding in crystalline cellulose I (Nishiyama et al., 2002, 2003).
[5] As proposed by Lee et al. (Lee et al., 2015).

S1. References

Bu, L., Himmel, M. E., & Crowley, M. F. (2015). The molecular origins of twist in cellulose I-beta. *Carbohydrate Polymers*, *125*, 146–152. http://dx.doi.org/10.1016/j.carbpol.2015.02.023

Fan, M., Dai, D., & Huang, B. (2012). Fourier Transform Infrared Spectroscopy for Natural Fibres. In S. Salih (Ed.), *Fourier Transform—Materials Analysis*. InTech. https://doi.org/10.5772/35482

Kondo, T., & Sawatari, C. (1996). A Fourier Transform Infra-Red Spectroscopic Analysis of the Character of Hydrogen Bonds in Amorphous Cellulose. *Polymer*, *37*(3), 393–399.

Lee, C. M., Kubicki, J. D., Fan, B., Zhong, L., Jarvis, M. C., & Kim, S. H. (2015). Hydrogen-Bonding Network and OH Stretch Vibration of Cellulose: Comparison of Computational Modeling with Polarized IR and SFG Spectra. *The Journal of Physical Chemistry B*, *119*(49), 15138–15149. https://doi.org/10.1021/acs.jpcb.5b08015

Liang, C. Y., & Marchessault, R. H. (1959). Infrared spectra of crystalline polysaccharides. I. Hydrogen bonds in native celluloses. *Journal of Polymer Science*, *37*(132), 385–395. https://doi.org/10.1002/pol.1959.1203713209

Marechal, Y., & Chanzy, H. (2000). The hydrogen bond network in Ib cellulose as observed by infrared spectrometry. *Journal of Molecular Structure*, 14.

Matthews, J. F., Skopec, C. E., Mason, P. E., Zuccato, P., Torget, R. W., Sugiyama, J., Himmel, M. E., & Brady, J. W. (2006). Computer simulation studies of microcrystalline cellulose I beta. *Carbohydrate Research*, *341*(1), 138–152. https://doi.org/10.1016/j.carres.2005.09.028

Nikonenko, N. A., Buslov, D. K., Sushko, N. I., & Zhbankov, R. G. (2000). *Investigation of stretching vibrations of glycosidic linkages in disaccharides and polysaccarides with use of IR spectra deconvolution*. *57*, 257–262.

Nishiyama, Y. (2009). Structure and properties of the cellulose microfibril. *Journal of Wood Science*, *55*(4), 241–249. https://doi.org/10.1007/s10086-009-1029-1

Nishiyama, Y., Langan, P., & Chanzy, H. (2002). Crystal Structure and Hydrogen-Bonding System in Cellulose I-Beta from Synchrotron X-ray and Neutron Fiber Diffraction. *Journal of the American Chemical Society*, *124*, 9074–9082.

Nishiyama, Y., Sugiyama, J., Chanzy, H., & Langan, P. (2003). Crystal structure and hydrogen bonding system in cellulose 1(alpha), from synchrotron X-ray and neutron fiber diffraction. *Journal of the American Chemical Society*, *125*(47), 14300–14306. https://doi.org/10.1021/ja037055w

O'Dell, P. J., Mudinoor, A. R., Parikh, S. J., & Jeoh, T. (2015). The Effect of Fibril Length and Architecture on the Accessibility of Reducing Ends of Cellulose Iα to *Trichoderma reesei* Cel7A. *Cellulose*, *22*(3), 1697–1713. https://doi.org/10.1007/s10570-015-0618-y

R. Stuart Tipson. (1968). *Infrared Spectroscopy of Carbohydrates: A review of the literature* [National Bureau of Standards Monograph 110]. United States Department of Commerce.

Schwanninger, M., Rodrigues, J. C., Pereira, H., & Hinterstoisser, B. (2004). Effects of short-time vibratory ball milling on the shape of FT-IR spectra of wood and cellulose. *Vibrational Spectroscopy*, *36*(1), 23–40. https://doi.org/10.1016/j.vibspec.2004.02.003

Shen, T. Y., & Gnanakaran, S. (2009). The Stability of Cellulose: A Statistical Perspective from a Coarse-Grained Model of Hydrogen-Bond Networks. *Biophysical Journal*, *96*(8), 3032–3040. https://doi.org/10.1016/j.bpj.2008.12.3953